https://doi.org/10.5194/gmd-2020-91
Preprint. Discussion started: 21 April 2020


Geoscientific Model Development Discussions

# A new distributed algorithm for routing network generation in model coupling and its evaluation based on C-Coupler2

Hao Yu[1], Li Liu[1], Chao Sun[1], Ruizhe Li[1], Xinzhu Yu[1], Cheng Zhang[1], Zhiyuan Zhang[2], Bin Wang[1,3]

[1] Ministry of Education Key Laboratory for Earth System Modeling, Department of Earth System Science, Tsinghua University, Beijing, China

[2] Hydro-Meteorological Center of Navy China, Beijing China

[3] State Key Laboratory of Numerical Modeling for Atmospheric Sciences and Geophysical Fluid Dynamics (LASG), Institute of Atmospheric Physics, Chinese Academy of Sciences, Beijing, China

*Correspondence to*: Li Liu (liuli-cess@tsinghua.edu.cn)

**Abstract.** It is a fundamental functionality of a coupler for Earth system modeling to efficiently handle data transfer between component models. Routing network generation is a major step for initializing the data transfer functionality. Most existing couplers employ an inefficient and unscalable global implementation for routing network generation that relies on collective communications. That's a main reason why the initialization cost of a coupler increases rapidly when using more processor cores. In this paper, we propose a new **D**istributed **a**lgorithm for **Ro**uting **n**etwork **g**eneration (DaRong), which does not introduce any collective communication and achieves much lower complexities than the global implementation. DaRong is of course much more efficient and scalable than the global implementation, which has been further demonstrated via empirical evaluations. DaRong has already been implemented in C-Coupler2. We believe that existing and future couplers can also benefit from it.

## 1 Introduction

A coupled model regarding Earth system Modelling generally highly depends on existing couplers (Hill et al., 2004; Craig et al., 2005; Larson et al., 2005; Balaji et al., 2006; Redler et al., 2010; Craig et al., 2012; Valcke, 2013; Liu et al., 2014; Hanke et al., 2016; Craig et al., 2017; Liu et al., 2018), each of which can combine different component models into a whole system and handle data interpolation between different model grids and data transfer between component models (Valcke, 2012). In response to more and more computation resulting from higher and higher resolutions in model development, the parallel efficiency of a coupled model on modern high-performance computers becomes more and more critical. Any module in a coupled model, including the coupler, can impact or even may damage the parallel efficiency of the whole coupled model. Although most existing couplers achieve scalable data transfer and data interpolation, i.e., the data transfer and data

https://doi.org/10.5194/gmd-2020-91
Preprint. Discussion started: 21 April 2020


Geoscientific Model Development Discussions

interpolation generally can be faster when using more processor cores, there is almost no evidence of scalable initialization of a coupler. Experiences from OASIS3-MCT and C-Coupler2 have revealed that the initialization cost of a coupler increases rapidly when using more processor cores (Craig et al., 2017; Liu et al., 2018). To achieve scalable initialization of couplers, this paper tries to make a first step through focusing on the initialization of data transfer.

The functionality of data transfer of couplers is transferring scalar variables or fields on a model grid (called gridded fields hereafter) from one component model to another via MPI (Message Passing Interface). A component model generally has been parallelized through decomposing the cells of a model grid into distinct subsets each of is assigned to an MPI process for cooperative concurrent computation, e.g., the sample parallel decompositions in Fig. 1a and 1b. To efficiently transfer gridded fields in parallel, Jacob et al. (2005) proposed an approach of *MxN* communication (called *MxN* approach) following the routing network where each pair of processes from the two component models should have a communication connection only when they have common grid cells (for example, Fig. 1c). This *MxN* approach has already been used in existing couplers for more than ten years. As the parallel decompositions of component models generally keep constant throughout the whole integration, a routing network can also keep constant. Thus, the *MxN* approach can be achieved with two major steps: generating the routing network when initializing the coupler, and transferring gridded fields based on the routing network throughout the coupled model integration. In spite of the scalability of the second major step, the first major step in existing couplers is unscalable, introducing higher cost when using more processor cores.

In this paper, we propose a new **D**istributed **a**lgorithm for **Ro**uting **n**etwork **g**eneration (DaRong), which is much faster and consumes much less memory than the existing approach. The remainder of this paper is organized as follows. We reveal the causes of unscalability of the existing implementations in Section 2, present and then evaluate DaRong in Section 3 and 4 respectively, and conclude this work in Section 5.

## 2 Existing implementations of routing network generation

In existing couplers, the global information of a parallel decomposition generally is distributed among all processes of a component model, where a process only records its local parallel decomposition corresponding to the grid cells assigned to it. Thus, almost all existing couplers use the following 4 steps for generating a routing network between the parallel decompositions of a source (*src*) and a destination (*dst*) component model.

1) Gathering global parallel decomposition: the *src*/*dst* root process gathers the global information of the *src*/*dst* parallel decomposition from all *src*/*dst* processes.
2) Exchanging global parallel decomposition: the *src*/*dst* root process first exchanges the *src*/*dst* global parallel decomposition with the *dst*/*src* root process, and then broadcasts the *dst*/*src* global parallel decomposition to all *src*/*dst*

https://doi.org/10.5194/gmd-2020-91
Preprint. Discussion started: 21 April 2020


Geoscientific Model Development Discussions

processes.

3) Detecting common grid cells: each *src*/*dst* process detects its common grid cells with each *dst*/*src* process based on its local parallel decomposition and the *dst*/*src* global parallel decomposition.
4) Generating the routing network: each *src*/*dst* process generates its local routing network according to the information about common grid cells.

Given that each of the *src* and *dst* component models uses $K$ processes and the corresponding grid size is $N$ (the grid has $N$ cells), the first and second steps correspond to collective communications with the time complexity of at least $O(N*logK)$ and the memory complexity of $O(N)$. Regarding the third step, the average time complexity corresponding to MCT (as well as CPL6/CPL7 and OASIS3-MCT that employ MCT for data transfer) on each *src*/*dst* process is $O(N*N/K)$, because the main loop of this step consists of two levels, i.e., the first level corresponds to the local parallel decomposition (the average number of cells in the local parallel decomposition is $N/K$) while the second level corresponds to the *dst*/*src* global parallel decomposition. The average time complexity of the third step corresponding to C-Coupler is $O(N)$, as C-Coupler first generates a map corresponding to the global parallel decomposition and next detects common cells based on looking up the map. Although this implementation can lower the time complexity, but introduces inefficient irregular memory accesses. As the last step does not depend on any global parallel decomposition, its average time complexity is $O(N/K)$.

Determined by the collective communications and the corresponding time complexity of $O(N*logK)$, and the time complexity of $O(N*N/K)$ or $O(N)$ corresponding to common grid cells detection, existing implementations of routing network generation are of course inefficient and unscalable under the increment of processor cores. Moreover, in response to the memory complexity of $O(N)$, more memory will be consumed when the model grids get finer.

In the following context, existing implementations of routing network generation are called global routing network generation.

## 3 Design and implementation

### 3.1 Overall design

Each cell of a grid can be numbered with a unique index from 1 to $N$ (called global cell index), while each grid cell assigned to the same process can also be numbered with a unique local cell index. Thus, the information of a given parallel decomposition can be recorded as a Cell Local-Global Mapping Table (CLGMT), each element of which is a triple of global

https://doi.org/10.5194/gmd-2020-91
Preprint. Discussion started: 21 April 2020


Geoscientific Model Development Discussions

cell index, process ID, and local cell index. For example, Tables 1 and 2 are the CLGMTs corresponding to the parallel decompositions in Fig. 1a and Fig. 1b respectively.

Generally, the CLGMT entries of a parallel decomposition are distributed among the processes of a component model, which means a process only stores a part of the CLGMT. The key idea of the existing global implementation can be summarized as reconstructing the global CLGMT of the peer parallel decomposition in each process for routing network generation. To be a scalable solution, DaRong should be fully based on distributed CLGMT without reconstructing any global CLGMT. The reason why existing implementations have to depend on global CLGMTs is because the distribution of the CLGMT entries is determined by a model and thus a coupler generally has to view any distribution as random.

Motivated by the above analysis, the key challenge to DaRong becomes how to efficiently rearrange the original distribution of the CLGMT entries of a given parallel decomposition into a regular intermediate distribution and how to efficiently generate the routing network based on the intermediate distribution. Specifically, we employ a regular intermediate distribution that evenly distributes the CLGMT entries among processes based on the ascending order of the global cell index. Such an intermediate distribution is not only simple, but also enables to easily achieve the rearrangement to the intermediate distribution via a sorting procedure similar to distributed sort. With the above preparations, DaRong is designed with the following major steps for generating a routing network between the *src* and *dst* component models:

1) The *src*/*dst* component model rearranges the original distribution of the CLGMT entries of the *src*/*dst* parallel decomposition into the regular intermediate distribution.
2) The *src* and *dst* component models exchange the CLGMT entries based on the intermediate distributions.
3) Each *src*/*dst* process generates table entries of the sharing relationship about how each grid cell is shared between the processes of the *src* and *dst* component models, based on the *src* and *dst* CLGMT entries on the intermediate distributions.
4) The *src*/*dst* component model rearranges the intermediate distribution of the entries of the sharing relationship table (SRT) into the original distribution of the CLGMT entries of the *src*/*dst* parallel decomposition.
5) Each *src*/*dst* process generates its local routing network based on the local SRT entries.

In the following context of this section, we will detail the implementation of each major step except the last one because it is similar to the last major step in the global implementation.

### 3.2 Rearranging CLGMT entries intra a component model

Such rearrangement is achieved via a divide-and-conquer sorting procedure that is similar to a merge sort with the keyword of global cell index. This procedure first sorts the CLGMT entries locally in each process, and next iteratively conducts distributed sort by a main loop of *logK* iterations (*K* is the number of processes of the *src*/*dst* component model). In an iteration,

https://doi.org/10.5194/gmd-2020-91
Preprint. Discussion started: 21 April 2020


processes are divided into distinct pairs and the two processes in each pair swap the CLGMT entries based on a point-to-point communication. Figure 2 shows an example of the distributed sort corresponding to the CLGMT entries in Table 1, and Table 3 shows the distributed CLGMT after rearranging the CLGMT entries in Table 2.

### 3.3 Exchanging CLGMT entries between component models

After the rearrangement of the CLGMT in a component model, the CLGMT entries are sorted in an ascending order of the global cell indexes and evenly distributed among processes. The CLGMT entries reserved in each process therefore have a determinate and non-overlapping range of global cell indexes, and such a range can be easily calculated from the grid size, the number of total processes, and process ID. Thus, it is easy to calculate the overlapping relationship of global cell index range between a *src* process and a *dst* process. As it is only necessary to exchange CLGMT entries between a pair of *src* and *dst* processes with overlapping ranges, point-to-point communications only are enough for handling the exchange of the CLGMT entries.

### 3.4 Generation of SRT

After the previous major step, each process reserves two sequences of CLGMT entries corresponding to the *src* and *dst* parallel decompositions respectively. Given that the two sequences contain *n1* and *n2* entries respectively, the time complexity of detecting the sharing relationship is $O(n1+n2)$, because the entries in each sequence have already been ordered in ascending global cell indexes, and a procedure similar to the kernel of merge sort that merges two ordered data sequences can handle such detection.

To record the sharing relationship, a SRT entry is designed as a quintuple of global cell index, *src* process ID, *src* local cell index, *dst* process ID, and *dst* local cell index. Given a quintuple $<q_1,q_2,q_3,q_4,q_5>$, it means that number $q_3$ local cell in number $q_2$ process of the *src* component model is number $q_1$ global cell, and the data on it will be transferred to number $q_5$ local cell in number $q_4$ process of the *dst* component model. Table 4 shows the SRT in the *src* component model, calculated from the rearranged distributed CLGMT entries in Fig. 2 and Table 3.

It is possible that multiple *src* CLGMT entries correspond to the same global cell index. Under such a case, any *src* CLGMT entry can be used for generating the corresponding SRT entries, because the *src* component model should guarantee that the data copies on the same grid cell are exactly the same. Given a *dst* CLGMT entry, if there is no *src* CLGMT entry with the same global cell index, no SRT entry will be generated. Given that multiple *dst* CLGMT entries correspond to the same global cell index and there is at least one *src* CLGMT entry with the same global cell index, a SRT entry will be generated for each *dst* CLGMT entry.

https://doi.org/10.5194/gmd-2020-91
Preprint. Discussion started: 21 April 2020


Geoscientific Model Development Discussions

### 3.5 Rearranging SRT entries intra a component model

After the previous major step, the SRT entries are distributed among processes of a component model according to the intermediate distribution. As a process can use only the SRT entries corresponding to its local cells for the last major step of local routing network generation, the SRT entries should be rearranged among the processes of a component model. We find that such rearrangement can also be achieved via a sorting procedure similar to the distributed sort with the keyword of *src*/*dst* process ID, or even the sorting procedure implemented for the first major step can be reused. Tables 5 and 6 show the SRT entries distributed in the *src* and *dst* component model respectively, after the rearrangement.

### 3.6 Time complexity and memory complexity

As DaRong does not reconstruct the global CLGMT, it only utilizes point-to-point communications and does not rely on any collective communication, and its average memory complexity is $O(N/K)$ on each process. As the implementation of its most time-consuming major steps are similar to a merge sort, and the time complexity of merge sort is $O(N*logN)$, the average time complexity of DaRong on each process is $O(N*(logN)/K)$, and average communication complexity is $O(N*(logK)/K)$.

To facilitate the implementation of the sorting procedure, we force the number of processes regarding the $1^{st} \sim 4^{th}$ major steps to be the maximum power of 2 ($2^n$) no larger than the total process number of the *src*/*dst* component model. For a process whose ID $I$ is not smaller than $2^n$, its CLGMT entries will be merged into the process with the ID of $I$-$2^n$ before the first major step, and the SPT entries corresponding to it will be obtained from the process with the ID of $I$-$2^n$ after the fourth major step. This strategy will not change the above time complexity and memory complexity of DaRong, as $2^n$ is larger than a half of the total process number.

## 4 Evaluation

For evaluating DaRong, we implemented it in C-Coupler2, which enables us to compare it with the original global routing network generation in C-Coupler2. We developed a toy coupled model consisting of two toy component models and C-Coupler2 for the evaluation, which enables us to flexibly change the model settings in terms of grid size and number of processor cores (processes). The toy coupled model is run on a supercomputer, where each computing node on the supercomputer includes two Intel Xeon E5-2678 v3 CPUs (Intel(R) Xeon(R) CPU (24 processor cores in total)), and all computing nodes were connected with an InfiniBand network. The codes were compiled by an Intel Fortran and C++ compiler

https://doi.org/10.5194/gmd-2020-91
Preprint. Discussion started: 21 April 2020


Geoscientific Model Development Discussions

at the optimization level O2, using an Intel MPI library (3.2.2). A maximum number of 3200 cores are used for running the toy coupled model.

We made an evaluation under the variation of process numbers (Fig. 3; two component models use the same number of processor cores). For the grid size of 500,000 (Fig. 3a), the execution time of DaRong does not really decrease when using more processor cores. This result is reasonable although it does not match the time complexity of DaRong. The communication complexity of DaRong is O(*N*(logK)/K*), where *logK* stands for the number of point-to-point communications in each process and *N*/*K* stands for the average message size in each communication. The average message size corresponding Fig. 3a is small (about 160KB under 60 cores while about 6KB under 1600 cores), while the execution time of point-to-point communication cannot keep linear to the message size and may be unstable when the message size is small. Different from DaRong, the execution time of the global implementation increases rapidly with the increment of core number. As a result, DaRong outperforms the global implementation more significantly when using more cores. When the grid size gets larger (e.g., 4,000,000 in Fig. 3b and 16,000,000 in Fig. 3c), DaRong still significantly outperforms the global implementation, while with better scalability.

Considering a model can use more processor cores for acceleration when its resolution gets finer, we further evaluated the weak scalability of DaRong, where we concurrently increased the grid size and core number to achieve similar numbers of grid points per process. As shown in Table 7, the execution time of DaRong increases slowly while the execution time of the global implementation increases rapidly with the increment of grid size and core number. This demonstrates that DaRong achieves much better weak scalability than the global implementation.

## 5 Conclusion

In this paper, we propose a new distributed algorithm, DaRong, for routing network generation. As it does not introduce any collective communication and achieves much lower complexity in terms of time, memory and communication than the global implementation that is widely used in existing couplers, it is of course much more efficient and scalable than the global implementation. The evaluation results further demonstrate this conclusion.

DaRong has already been implemented in C-Coupler2. Its code is publicly available in a C-Coupler2 version and will be further used in future C-Coupler versions. We do believe that existing couplers can also benefit from DaRong, for accelerating routing the network generation as well as the initialization of couplers.

*Code availability.* The source code of DaRong can be viewed and run with C-Coupler2 and the toy coupled model via https://doi.org/10.5281/zenodo.3753217.

https://doi.org/10.5194/gmd-2020-91
Preprint. Discussion started: 21 April 2020


Geoscientific Model Development Discussions

*Author contributions.* HY was responsible for code development, software testing and experimental evaluation of DaRong, and co-led paper writing. LL initiated this research, was responsible for the motivation and design of DaRong, supervised HY, and co-led paper writing. CS, RL, XY and CZ contributed to code development and software testing. ZZ and BW contributed to the motivation and software testing. All authors contributed to improvement of ideas and paper writing.

*Competing interests.* The authors declare that they have no conflict of interest.

*Acknowledgements*. This work was jointly supported in part by the National Key Research Project of China (grant no. 2017YFC1501903).

**References**

Balaji, V., J. Anderson, I. Held, M. Winton, J. Durachta, S. Malyshev, and R. J. Stouffer, 2006: The Exchange Grid: a mechanism for data exchange between Earth System components on independent grids. In: Proceedings of the 2005 International Conference on Parallel Computational Fluid Dynamics, College Park, MD, USA, Elsevier, 2006.

Craig, A. P., M. Vertenstein, and R. Jacob, 2012: A New Flexible Coupler for Earth System Modelling developed for CCSM4 and CESM1. Int. J. High Perform. C, 26-1, 31–42, doi:10.1177/1094342011428141.

Craig, A. P., R. L. Jacob, B. Kauffman, T. Bettge, J. W. Larson, E. T. Ong, C. H. Q. Ding, Y. He, 2005: CPL6: The New Extensible, High Performance Parallel Coupler for the Community Climate System Model. International Journal of High Performance Computing Applications, 19(3): 309-327.

Craig, A., Valcke, S., and Coquart, L.: Development and performance of a new version of the OASIS coupler, OASIS3-MCT_3.0, Geosci. Model Dev., 10, 3297-3308, https://doi.org/10.5194/gmd-10-3297-2017, 2017

Hanke, M., Redler, R., Holfeld, T., and Yastremsky, M.: YAC 1.2.0: new aspects for coupling software in Earth system modelling, Geosci. Model Dev., 9, 2755–2769, https://doi.org/10.5194/gmd-9-2755-2016, 2016

Hill, C., C. DeLuca, V. Balaji, M. Suarez, and A. da Silva, 2004: Architecture of the Earth System Modelling Framework. Comput. Sci. Eng., 6, 18–28.

Jacob, R., J. Larson, and E. Ong, 2005: M x N Communication and Parallel Interpolation in Community Climate System Model Version 3 Using the Model Coupling Toolkit, Int. J. High. Perform. C, 19, 293–307.

Larson, J., R. Jacob, and E. Ong, 2005: The Model Coupling Toolkit: A New Fortran90 Toolkit for Building Multiphysics Parallel Coupled Models. Int. J. High Perform, C, 19, 277–292.

Liu, L., Yang, G., Wang, B., Zhang, C., Li, R., Zhang, Z., Ji, Y., and Wang, L.: C-Coupler1: a Chinese community coupler for Earth system modeling, Geosci. Model Dev., 7, 2281-2302, doi:10.5194/gmd-7-2281-2014, 2014.

https://doi.org/10.5194/gmd-2020-91
Preprint. Discussion started: 21 April 2020




Liu, L., Zhang, C., Li, R., Wang, B., and Yang, G.: C-Coupler2: a flexible and user-friendly community coupler for model coupling and nesting, Geosci. Model Dev., 11, 3557-3586, https://doi.org/10.5194/gmd-11-3557-2018, 2018.

R. Redler, S. Valcke and H. Ritzdorf. OASIS4 - a coupling software for next generation earth system modeling. Geosci. Model Dev., 2010, 3(1): 87~104.

Valcke, S., 2013: The OASIS3 coupler: A European climate modelling community software. Geosci. Model Dev., 6, 373–388, doi:10.5194/gmd-6–373-2013

Valcke, S., Balaji, V., Craig, A., Deluca, C., Dunlap, R., Ford, R. W., Jacob, R., Larson, J., Okuinghttons, R., Riley, G., Vertenstein, M: Coupling technologies for Earth System Modelling, Geosci. Model Dev., 5, 1589-1596, 2012.

https://doi.org/10.5194/gmd-2020-91
Preprint. Discussion started: 21 April 2020


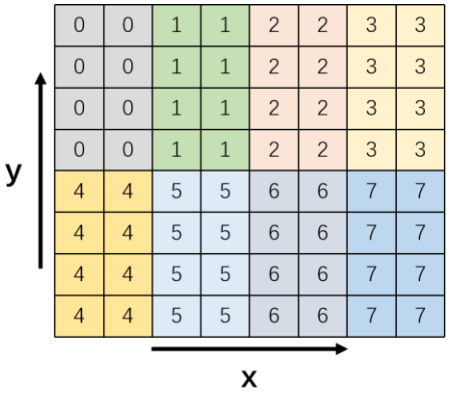


(a) A regular 2-D parallel decomposition in both X and Y direction

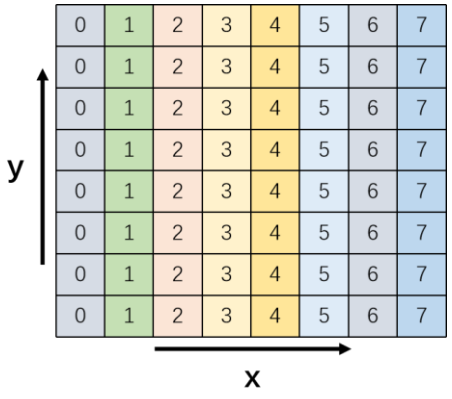


(b) A regular 1-D parallel decomposition in only X direction

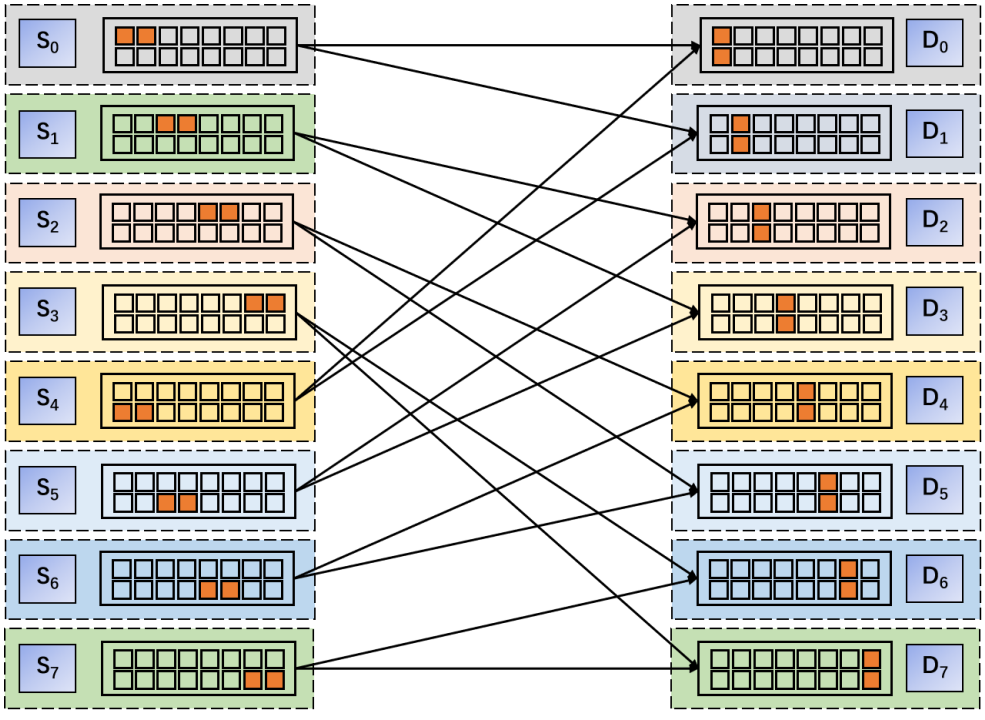


(c) The routing network from the parallel decomposition in Fig. 1a (**S**ource) to the parallel decomposition in Fig. 1(b) (**D**estination).

**Figure 1. Two sample parallel decompositions of an 8x8 grid under 8 processes (Fig. 1a and 1b) and the routing network between them (Fig. 1c). Each colour corresponds to a process)**

https://doi.org/10.5194/gmd-2020-91
Preprint. Discussion started: 21 April 2020


Geoscientific Model Development Discussions

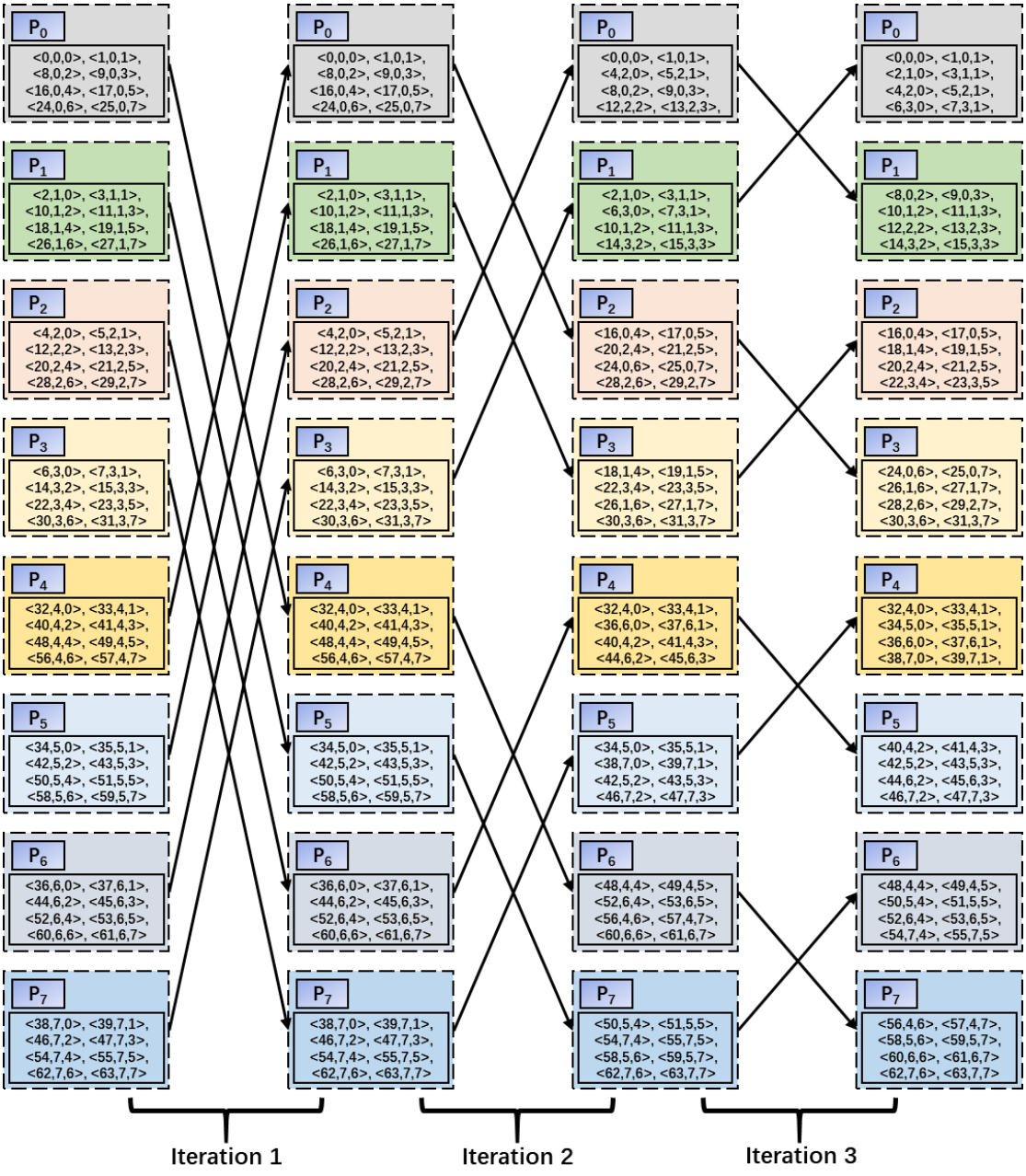


**Figure 2. The distributed sort corresponding to the CLGMT entries in Table 1. Each iteration makes the CLGMT entries with larger global cell indexes reserved in the processes with larger IDs. For example, after the first iteration, the CLGMT entries with global cell indexes between 0 and 31 are reserved in P0~P3, while the remaining CLGMT entries are reserved in P4~P7.**

https://doi.org/10.5194/gmd-2020-91
Preprint. Discussion started: 21 April 2020


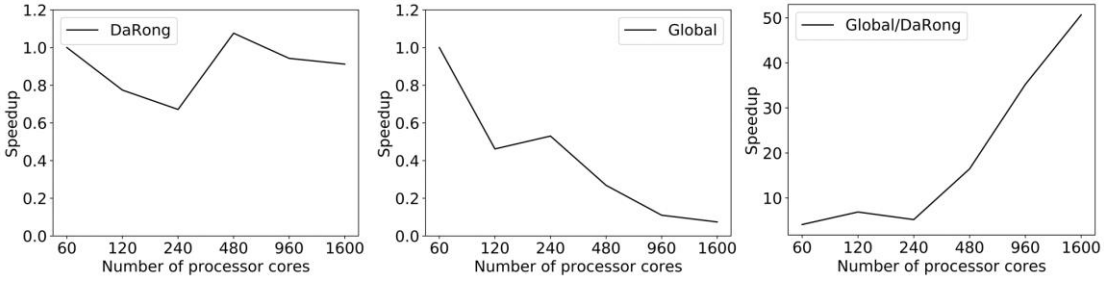


(a) Speedups under the grid size of 500,000. The execution time of DaRong and the global under 60 cores is 0.031 s and 0.129 s respectively.

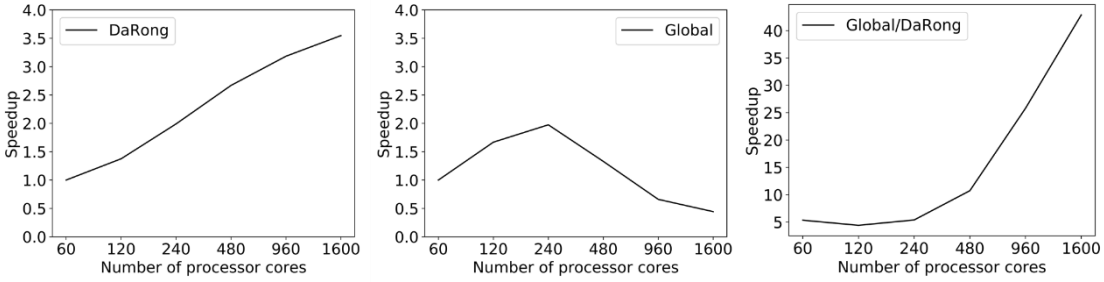


(b) Speedups under the grid size of 4,000,000. The execution time of DaRong and the global under 60 cores is 0.161 s and 0.863 s respectively.

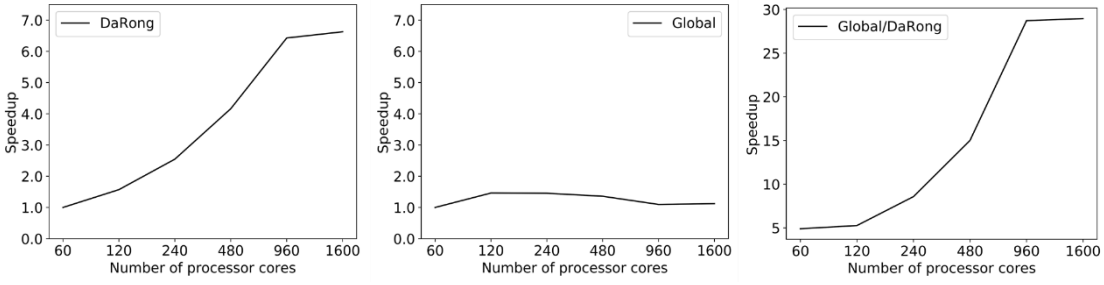


(c) Speedups under the grid size of 16,000,000. The execution time of DaRong and the global under 60 cores is 0.702 s and 3.44 s respectively.

**Figure 3. Performance of DaRong and the comparison with the original global routing network generation (Global) under different core numbers and grid sizes. Two toy component models use the same number of processor cores in each test case. The speedup in the left or middle graph of each sub figure is used for evaluating the scalability of DaRong or the global when increasing processor cores. It is the ratio between the execution time under 60 cores and the execution time under another core number. The speedup in the right graph of each sub figure is the ratio of the execution time between the global and DaRong, and bigger speedup means that is DaRong is faster.**

https://doi.org/10.5194/gmd-2020-91
Preprint. Discussion started: 21 April 2020


Geoscientific Model Development Discussions

285 **Table 1. The Cell Local-Global Mapping Table (CLGMT) of the parallel decomposition in Fig. 1a**

| Process ID | Cell Local-Global Mapping Table entries |
|---|---|
| 0 | <0,0,0>, <1,0,1>, <8,0,2>, <9,0,3>, <16,0,4>, <17,0,5>, <24,0,6>, <25,0,7> |
| 1 | <2,1,0>, <3,1,1>, <10,1,2>, <11,1,3>, <18,1,4>, <19,1,5>, <26,1,6>, <27,1,7> |
| 2 | <4,2,0>, <5,2,1>, <12,2,2>, <13,2,3>, <20,2,4>, <21,2,5>, <28,2,6>, <29,2,7> |
| 3 | <6,3,0>, <7,3,1>, <14,3,2>, <15,3,3>, <22,3,4>, <23,3,5>, <30,3,6>, <31,3,7> |
| 4 | <32,4,0>, <33,4,1>, <40,4,2>, <41,4,3>, <48,4,4>, <49,4,5>, <56,4,6>, <57,4,7> |
| 5 | <34,5,0>, <35,5,1>, <42,5,2>, <43,5,3>, <50,5,4>, <51,5,5>, <58,5,6>, <59,5,7> |
| 6 | <36,6,0>, <37,6,1>, <44,6,2>, <45,6,3>, <52,6,4>, <53,6,5>, <60,6,6>, <61,6,7> |
| 7 | <38,7,0>, <39,7,1>, <46,7,2>, <47,7,3>, <54,7,4>, <55,7,5>, <62,7,6>, <63,7,7> |

https://doi.org/10.5194/gmd-2020-91
Preprint. Discussion started: 21 April 2020


Geoscientific Model Development Discussions

**Table 2. The Cell Local-Global Mapping Table (CLGMT) of the parallel decomposition in Fig. 1b**

| Process ID | Cell Local-Global Mapping Table entries |
|---|---|
| 0 | <0,0,0>, <8,0,1>, <16,0,2>, <24,0,3>, <32,0,4>, <40,0,5>, <48,0,6>, <56,0,7> |
| 1 | <1,1,0>, <9,1,1>, <17,1,2>, <25,1,3>, <33,1,4>, <41,1,5>, <49,1,6>, <57,1,7> |
| 2 | <2,2,0>, <10,2,1>, <18,2,2>, <26,2,3>, <34,2,4>, <42,2,5>, <50,2,6>, <58,2,7> |
| 3 | <3,3,0>, <11,3,1>, <19,3,2>, <27,3,3>, <35,3,4>, <43,3,5>, <51,3,6>, <59,3,7> |
| 4 | <4,4,0>, <12,4,1>, <20,4,2>, <28,4,3>, <36,4,4>, <44,4,5>, <52,4,6>, <60,4,7> |
| 5 | <5,5,0>, <13,5,1>, <21,5,2>, <29,5,3>, <37,5,4>, <45,5,5>, <53,5,6>, <61,5,7> |
| 6 | <6,6,0>, <14,6,1>, <22,6,2>, <30,6,3>, <38,6,4>, <46,6,5>, <54,6,6>, <62,6,7> |
| 7 | <7,7,0>, <15,7,1>, <23,7,2>, <31,7,3>, <39,7,4>, <47,7,5>, <55,7,6>, <63,7,7> |

https://doi.org/10.5194/gmd-2020-91
Preprint. Discussion started: 21 April 2020


Geoscientific Model Development Discussions

**Table 3. The distributed CLGMT after rearranging the CLGMT entries in Table 2**

| Process ID | CLGMT entries |
|---|---|
| 0 | <0,0,0>, <1,1,0>, <2,2,0>, <3,3,0>, <4,4,0>, <5,5,0>, <6,6,0>, <7,7,0> |
| 1 | <8,0,1>, <9,1,1>, <10,2,1>, <11,3,1>, <12,4,1>, <13,5,1>, <14,6,1>, <15,7,1> |
| 2 | <16,0,2>, <17,1,2>, <18,2,2>, <19,3,2>, <20,4,2>, <21,5,2>, <22,6,2>, <23,7,2> |
| 3 | <24,0,3>, <25,1,3>, <26,2,3>, <27,3,3>, <28,4,3>, <29,5,3>, <30,6,3>, <31,7,3> |
| 4 | <32,0,4>, <33,1,4>, <34,2,4>, <35,3,4>, <36,4,4>, <37,5,4>, <38,6,4>, <39,7,4> |
| 5 | <40,0,5>, <41,1,5>, <42,2,5>, <43,3,5>, <44,4,5>, <45,5,5>, <46,6,5>, <47,7,5> |
| 6 | <48,0,6>, <49,1,6>, <50,2,6>, <51,3,6>, <52,4,6>, <53,5,6>, <54,6,6>, <55,7,6> |
| 7 | <56,0,7>, <57,1,7>, <58,2,7>, <59,3,7>, <60,4,7>, <61,5,7>, <62,6,7>, <63,7,7> |

290

https://doi.org/10.5194/gmd-2020-91
Preprint. Discussion started: 21 April 2020


Geoscientific Model Development Discussions

**Table 4. The Sharing Relationship Table (SRT) calculated from the rearranged distributed CLGMT entries in Fig. 2 and Table 3.**

| Process ID | Sharing Relationship Table entries |
|---|---|
| 0 | <0,0,0,0,0>, <1,0,1,1,0>, <2,1,0,2,0>, <3,1,1,3,0>, <4,2,0,4,0>, <5,2,1,5,0>, <6,3,0,6,0>, <7,3,1,7,0> |
| 1 | <8,0,2,0,1>, <9,0,3,1,1>, <10,1,2,2,1>, <11,1,3,3,1>, <12,2,2,4,1>, <13,2,3,5,1>, <14,3,2,6,1>, <15,3,3,7,1> |
| 2 | <16,0,4,0,2>, <17,0,5,1,2>, <18,1,4,2,2>, <19,1,5,3,2>, <20,2,4,4,2>, <21,2,5,5,2>, <22,3,4,6,2>, <23,3,5,7,2> |
| 3 | <24,0,6,0,3>, <25,0,7,1,3>, <26,1,6,2,3>, <27,1,7,3,3>, <28,2,6,4,3>, <29,2,7,5,3>, <30,3,6,6,3>, <31,3,7,7,3> |
| 4 | <32,4,0,0,4>, <33,4,1,1,4>, <34,5,0,2,4>, <35,5,1,3,4>, <36,6,0,4,4>, <37,6,1,5,4>, <38,7,0,6,4>, <39,7,1,7,4> |
| 5 | <40,4,2,0,5>, <41,4,3,1,5>, <42,5,2,2,5>, <43,5,3,3,5>, <44,6,2,4,5>, <45,6,3,5,5>, <46,7,2,6,5>, <47,7,3,7,5> |
| 6 | <48,4,4,0,6>, <49,4,5,1,6>, <50,5,4,2,6>, <51,5,5,3,6>, <52,6,4,4,6>, <53,6,5,5,6>, <54,7,4,6,6>, <55,7,5,7,6> |
| 7 | <56,4,6,0,7>, <57,4,7,1,7>, <58,5,6,2,7>, <59,5,7,3,7>, <60,6,6,4,7>, <61,6,7,5,7>, <62,7,6,6,7>, <63,7,7,7,7> |

https://doi.org/10.5194/gmd-2020-91
Preprint. Discussion started: 21 April 2020


Geoscientific Model Development Discussions

**Table 5. The SRT entries distributed in the *src* component model after rearranging the SRT in Table 4**

| Process ID | Sharing Relationship Table entries |
|---|---|
| 0 | <0,0,0,0,0>, <1,0,1,1,0>, <8,0,2,0,1>, <9,0,3,1,1>, <16,0,4,0,2>, <17,0,5,1,2>, <24,0,6,0,3>, <25,0,7,1,3> |
| 1 | <2,1,0,2,0>, <3,1,1,3,0>, <10,1,2,2,1>, <11,1,3,3,1>, <18,1,4,2,2>, <19,1,5,3,2>, <26,1,6,2,3>, <27,1,7,3,3> |
| 2 | <4,2,0,4,0>, <5,2,1,5,0>, <12,2,2,4,1>, <13,2,3,5,1>, <20,2,4,4,2>, <21,2,5,5,2>, <28,2,6,4,3>, <29,2,7,5,3> |
| 3 | <6,3,0,6,0>, <7,3,1,7,0>, <14,3,2,6,1>, <15,3,3,7,1>, <22,3,4,6,2>, <23,3,5,7,2>, <30,3,6,6,3>, <31,3,7,7,3> |
| 4 | <32,4,0,0,4>, <33,4,1,1,4>, <40,4,2,0,5>, <41,4,3,1,5>, <48,4,4,0,6>, <49,4,5,1,6>, <56,4,6,0,7>, <57,4,7,1,7> |
| 5 | <34,5,0,2,4>, <35,5,1,3,4>, <42,5,2,2,5>, <43,5,3,3,5>, <50,5,4,2,6>, <51,5,5,3,6>, <58,5,6,2,7>, <59,5,7,3,7> |
| 6 | <36,6,0,4,4>, <37,6,1,5,4>, <44,6,2,4,5>, <45,6,3,5,5>, <52,6,4,4,6>, <53,6,5,5,6>, <60,6,6,4,7>, <61,6,7,5,7> |
| 7 | <38,7,0,6,4>, <39,7,1,7,4>, <46,7,2,6,5>, <47,7,3,7,5>, <54,7,4,6,6>, <55,7,5,7,6>, <62,7,6,6,7>, <63,7,7,7,7> |

295

https://doi.org/10.5194/gmd-2020-91
Preprint. Discussion started: 21 April 2020


Geoscientific Model Development Discussions

**Table 6. The SRT entries distributed in the *dst* component model after rearranging the SRT in Table 4**

| Process ID | Sharing Relationship Table entries |
|---|---|
| 0 | <0,0,0,0,0>, <8,0,2,0,1>, <16,0,4,0,2>, <24,0,6,0,3>, <32,4,0,0,4>, <40,4,2,0,5>, <48,4,4,0,6>, <56,4,6,0,7> |
| 1 | <1,0,1,1,0>, <9,0,3,1,1>, <17,0,5,1,2>, <25,0,7,1,3>, <33,4,1,1,4>, <41,4,3,1,5>, <49,4,5,1,6>, <57,4,7,1,7> |
| 2 | <2,1,0,2,0>, <10,1,2,2,1>, <18,1,4,2,2>, <26,1,6,2,3>, <34,5,0,2,4>, <42,5,2,2,5>, <50,5,4,2,6>, <58,5,6,2,7> |
| 3 | <3,1,1,3,0>, <11,1,3,3,1>, <19,1,5,3,2>, <27,1,7,3,3>, <35,5,1,3,4>, <43,5,3,3,5>, <51,5,5,3,6>, <59,5,7,3,7> |
| 4 | <4,2,0,4,0>, <12,2,2,4,1>, <20,2,4,4,2>, <28,2,6,4,3>, <36,6,0,4,4>, <44,6,2,4,5>, <52,6,4,4,6>, <60,6,6,4,7> |
| 5 | <5,2,1,5,0>, <13,2,3,5,1>, <21,2,5,5,2>, <29,2,7,5,3>, <37,6,1,5,4>, <45,6,3,5,5>, <53,6,5,5,6>, <61,6,7,5,7> |
| 6 | <6,3,0,6,0>, <14,3,2,6,1>, <22,3,4,6,2>, <30,3,6,6,3>, <38,7,0,6,4>, <46,7,2,6,5>, <54,7,4,6,6>, <62,7,6,6,7> |
| 7 | <7,3,1,7,0>, <15,3,3,7,1>, <23,3,5,7,2>, <31,3,7,7,3>, <39,7,1,7,4>, <47,7,3,7,5>, <55,7,5,7,6>, <63,7,7,7,7> |

https://doi.org/10.5194/gmd-2020-91
Preprint. Discussion started: 21 April 2020


Geoscientific Model Development Discussions

**Table 7. Performance of DaRong and the comparison with the original global routing network generation (Global) when concurrently increasing the grid size and core number.**

| Core number | Grid size | Execution time (s) of DaRong | Execution time (s) of Global | Global/DaRong |
|---|---|---|---|---|
| 250 | 500,000 | 0.032 | 0.262 | 8.19 |
| 450 | 1,000,000 | 0.034 | 0.492 | 14.47 |
| 900 | 2,000,000 | 0.041 | 1.158 | 28.24 |
| 1600 | 4,000,000 | 0.045 | 1.949 | 43.31 |

300